Developmental Cell
Article

Regulation of Floral Patterning by Flowering Time Genes

Chang Liu,[1] Wanyan Xi,[1,2] Lisha Shen,[1,2] Caiping Tan,[1] and Hao Yu[1,*]
[1]Department of Biological Sciences and Temasek Life Sciences Laboratory, National University of Singapore, 10 Science Drive 4, 117543, Singapore
[2]These authors contributed equally to this work
*Correspondence: dbsyuhao@nus.edu.sg
DOI 10.1016/j.devcel.2009.03.011

SUMMARY

Floral patterning in *Arabidopsis* requires activation of floral homeotic genes by the floral meristem identity gene, *LEAFY* (*LFY*). Here we show that precise activation of expression of class B and C homeotic genes in floral meristems is regulated by three flowering time genes, *SHORT VEGETATIVE PHASE* (*SVP*), *SUPPRESSOR OF OVEREXPRESSION OF CONSTANS 1* (*SOC1*), and *AGAMOUS-LIKE 24* (*AGL24*), through direct control of a *LFY* coregulator, *SEPALLATA3* (*SEP3*). Orchestrated repression of *SEP3* by SVP, AGL24, and SOC1 is mediated by recruiting two interacting chromatin regulators, TERMINAL FLOWER 2/LIKE HETEROCHROMATIN PROTEIN 1 and SAP18, a member of SIN3 histone deacetylase complex. Our finding of coordinated regulation of *SEP3* by flowering time genes reveals a hitherto unknown genetic pathway that prevents premature differentiation of floral meristems and determines the appropriate timing of floral organ patterning.

INTRODUCTION

Although flowers generated from different plant species are extensively diversified, the underlying genetic and molecular mechanisms that regulate flower development are highly conserved. In *Arabidopsis*, our understanding of the mechanisms controlling flower development are encapsulated in the "ABC" model, which describes how each whorl of floral organs is determined by a combinatorial action of the A, B, and C class floral homeotic genes (Bowman et al., 1991; Coen and Meyerowitz, 1991). Further discovery of the *SEPALLATA* (*SEP*) genes has led to a revised "ABCE" model, in which the E class *SEP* genes function redundantly with other homeotic genes in specifying floral organs (Ditta et al., 2004; Goto et al., 2001; Pelaz et al., 2000; Theissen and Saedler, 2001).

A key regulator of early floral patterning is the floral meristem identity gene, *LEAFY* (*LFY*), which is expressed throughout young floral meristems and activates various floral homeotic genes in combination with other regulators (Parcy et al., 1998; Weigel et al., 1992). *LFY* directly activates *APETALA1* (*AP1*), which plays dual roles in specifying the floral meristem and acting as a class A gene to determine the identity of perianth organs (Mandel et al., 1992; Wagner et al., 1999). Activation of a class B gene, *APETALA3* (*AP3*), which determines petals and stamens, requires the concerted action of *LFY*, *AP1*, and *UNUSUAL FLORAL ORGANS*, an F box gene (Ng and Yanofsky, 2001; Parcy et al., 1998). *LFY* also cooperates with a homeobox gene, *WUSCHEL* (*WUS*), to activate the class C gene, *AGAMOUS* (*AG*), which specifies the identity of stamens and carpels (Lenhard et al., 2001; Lohmann et al., 2001). These observations have demonstrated an indispensable role of *LFY* in mediating early floral patterning, which leads to the spatially restricted expression of floral homeotic genes described in the ABC model.

Although the expression of class B and C genes is reduced in *lfy-6* null mutants, their expression is not abolished (Weigel and Meyerowitz, 1993), indicating that some other factors may also contribute to activation of floral homeotic genes. In this study, we report that a genetic pathway mediated by three flowering time genes, *SHORT VEGETATIVE PHASE* (*SVP*), *SUPPRESSOR OF OVEREXPRESSION OF CONSTANS 1* (*SOC1*), and *AGAMOUS-LIKE 24* (*AGL24*), is required for the regulation of early floral patterning in *Arabidopsis*. These three genes encode closely related MADS box transcription factors involved in the control of flowering time (Hartmann et al., 2000; Lee et al., 2000; Michaels et al., 2003; Yu et al., 2002). In the emerging floral meristems, the expression of these genes is normally downregulated by *AP1* to prevent the reversion of floral meristems into various shoot structures (Liu et al., 2007; Yu et al., 2004). Their single and double mutants produce normal flowers under standard growth temperature except for *svp-41 agl24-2*, in which several flowers at basal positions of the inflorescence show mild floral defects (Gregis et al., 2006). The defects are enhanced by growing at a higher temperature (e.g., 30°C) or in the background of *ap1* mutants, indicating the involvement of *AP1* and these flowering time genes in flower development.

By investigating dramatic floral defects in the triple mutant *soc1-2 agl24-1 svp-41*, we have found that these three flowering time genes control floral patterning by directly preventing the ectopic expression of *SEP3*, a member of the class E genes, which acts with *LFY* to activate class B and C gene expression in stage 3 floral meristems. To maintain *SEP3* chromatin in a silenced state, SVP interacts with TERMINAL FLOWER 2/LIKE HETEROCHROMATIN PROTEIN 1 (TFL2/LHP1) to modulate trimethylation of histone H3 lysine 27 (H3K27me3), while SOC1 and AGL24 interact with SAP18, a member of Sin3/histone deacetylase (HDAC) complex, to modulate histone H3 acetylation. Our results suggest that orchestrated repression of *SEP3* by flowering time genes prevents premature differentiation of

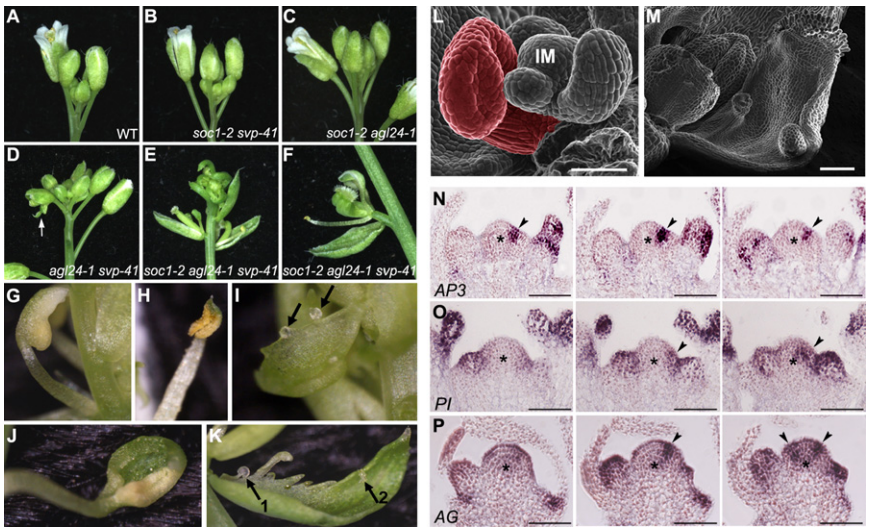

Figure 1. Floral Defects of *soc1-2 agl24-1 svp-41*

(A–E) Inflorescence apex of wild-type (A), *soc1-2 svp-41* (B), *soc1-2 agl24-1* (C), *agl24-1 svp-41* (D), and *soc1-2 agl24-1 svp-41* (E) plants. Arrow indicates a deformed petal in *agl24-1 svp-41*.

(F) Each *soc1-2 agl24-1 svp-41* floral structure is subtended by a bract.

(G–K) Homeotic transformation of floral organs in *soc1-2 agl24-1 svp-41*. (G) A petaloid stamen. (H) A stamen with a green tip. (I) A carpelloid sepal. Arrows indicate ovules on the edge. (J) A sepaloid stamen. Note that the locule is only partially developed. (K) A carpelloid bract with an ovule (arrow 1) and stigmatic tissue (arrow 2) on its edge.

(L and M) Scanning electron micrograph analysis of an inflorescence apex (L) and a carpelloid sepal with ovules and stigmas (M) of *soc1-2 agl24-1 svp-41*. (L) A stamen highlighted in red directly emerges from the inflorescence meristem (IM). Scale bars, 100 μm.

(N–P) In situ hybridization showing ectopic expression of *AP3* (N), *PI* (O), and *AG* (P) in serial sections of an inflorescence apex of *soc1-2 agl24-1 svp-41*. Arrowheads indicate their ectopic expression in floral anlagen. Asterisks indicate inflorescence meristems. Scale bars, 100 μm.

floral meristems and determines the timing of floral organ patterning.

RESULTS

SOC1, *AGL24*, and *SVP* Redundantly Regulate Flower Development

Our previous study on flowering time genes led to the generation of various combinations of mutants among *soc1-2*, *agl24-1*, and *svp-41* (Li et al., 2008). Among all the single and double mutants generated, only flowers of *agl24-1 svp-41* showed mild defects, including slightly reduced floral organs and occasional generation of deformed petals at the standard growth temperature (22°C) (Figures 1A–1D; see Table S1 available online), which was consistent with a previous observation (Gregis et al., 2006). However, the triple mutant *soc1-2 agl24-1 svp-41* exhibited striking floral defects with loss of most floral organs and generation of various chimeric floral structures (Figures 1E and 1G–1M; Table S1). The severity of these phenotypes increased acropetally. In addition, each floral structure in *soc1-2 agl24-1 svp-41* was subtended by a bract (Figure 1F). The floral phenotypes of *soc1-2 agl24-1 svp-41* were rescued by the transgene containing any genomic fragment of *SOC1*, *AGL24*, or *SVP* (Figure S1), suggesting that these genes play redundant roles in regulating flower development.

Class B and C Genes Are Deregulated in *soc1-2 agl24-1 svp-41*

To examine whether the floral defects in *soc1-2 agl24-1 svp-41* are due to deregulation of floral homeotic genes, we performed in situ hybridization to detect the expression of floral homeotic genes in inflorescence apices. For class A genes, *APETALA2* (*AP2*) was expressed in a pattern similar to that in wild-type plants, while *AP1* exhibited a similar expression pattern but with slightly reduced intensity (Figure S2), which is probably due to the repression by ectopic *AG* activity (see below) (Gustafson-Brown et al., 1994). However, two class B genes, *AP3* and *PISTILLATA* (*PI*), and one class C gene, *AG*, were all ectopically expressed in floral anlagen in the inflorescence meristem and irregularly expressed in emerging floral meristems before stage 3 (Figures 1N–1P) (Smyth et al., 1990). This is in great contrast to their expression in wild-type plants, where they start to be expressed in stage 3 floral meristems (Goto and Meyerowitz, 1994; Jack et al., 1992; Yanofsky et al., 1990). Such deregulation of class B and C homeotic genes was not observed in the double mutants (data not shown), suggesting that *SOC1*, *SVP*, and *AGL24* redundantly control the expression of class B and C genes in young floral meristems before floral patterning occurs.

We further investigated whether class B and C genes are regulated by *SOC1*, *SVP*, and *AGL24* in other developmental contexts. In *soc1-2 agl24-1 svp-41*, neither class B nor C genes were ectopically expressed during the vegetative phase, but they appeared in stage 1 floral meristems immediately after floral transition (Figure 2A). This indicates that deregulation of class B and C genes in *soc1-2 agl24-1 svp-41* coincides with the reproductive growth. Interestingly, as the inflorescences of *soc1-2 agl24-1 svp-41* bolted, ectopic *AP3* expression remained mostly unchanged, whereas the domain and intensity of ectopic *AG* expression gradually increased in inflorescence apices (Figure S3). Such an expression profile was consistent with the observation that carpelloid structures increased acropetally in the inflorescences of the triple mutants (Table S1).

As carpelloid structures and homeotic transformation of sepals into petals were still observed in *soc1-2 agl24-1 svp-41 ap3-3* and *soc1-2 agl24-1 svp-41 ag-1*, respectively (Figure S4), deregulation of class B and C genes in *soc1-2 agl24-1 svp-41* was at least partially independent of each other. These results, together with the observation of concurrent activation of class B and C genes in *soc1-2 agl24-1 svp-41* (Figure 2A; Figure S3), imply that a synchronized mechanism mediated by these flowering time

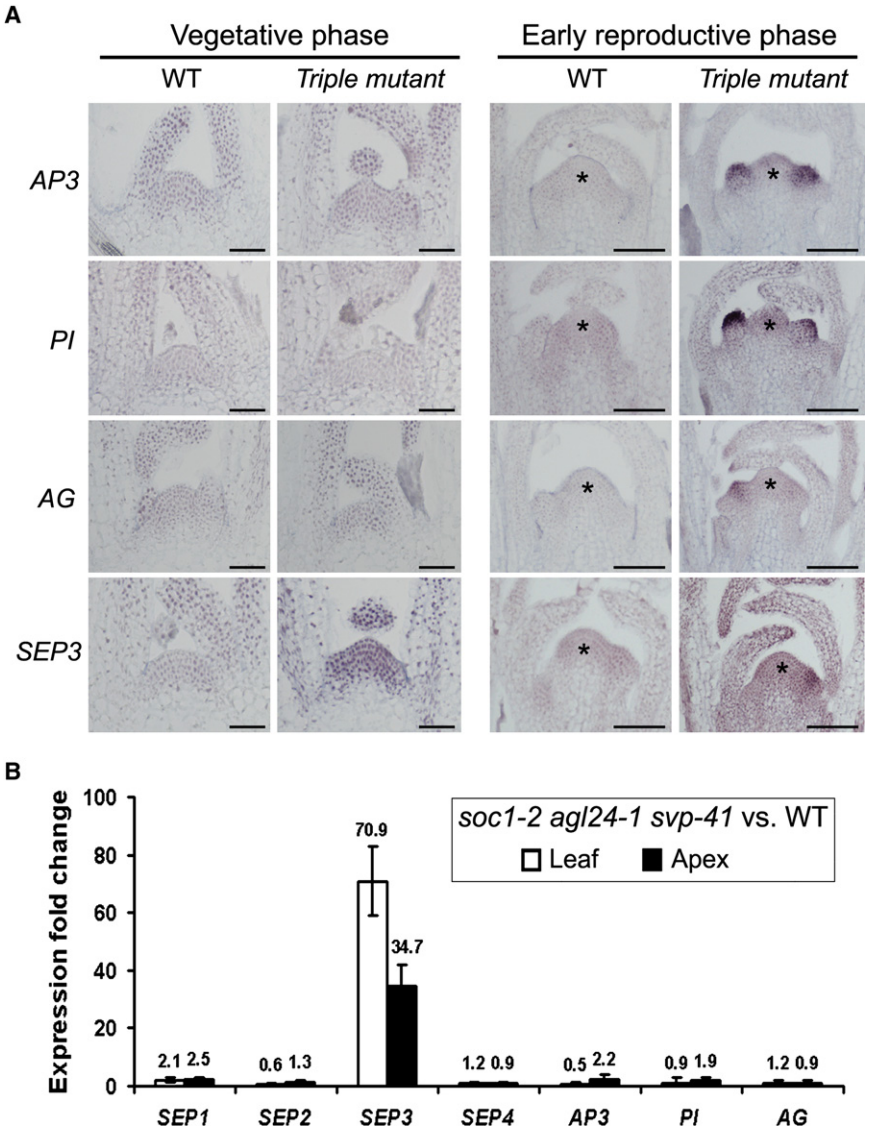

Figure 2. Ectopic Expression of Floral Homeotic Genes in *soc1-2 agl24-1 svp-41*

(A) In situ localization of floral homeotic genes at shoot apices of wild-type and *soc1-2 agl24-1 svp-41* plants during the vegetative and early reproductive stages. Asterisks indicate inflorescence meristems. Scale bars, 50 μm (vegetative apices); 100 μm (reproductive apices).

(B) Fold change of the expression of floral homeotic genes in 9-day-old *soc1-2 agl24-1 svp-41* against that in wild-type seedlings. Cotyledons and rosette leaves including petioles were collected as "Leaf," while the other aerial tissues were collected as "Apex." The average value of fold change is shown above each column. Error bars indicate SD.

genes could regulate both class B and C genes in floral meristems. Since chromatin immunoprecipitation (ChIP) assays did not reveal binding of SOC1, SVP, and AGL24 to the promoters of class B and C genes (Figure S5), their interaction could be mediated by other intermediate factor(s).

SEP3 Is Repressed by *SOC1*, *AGL24*, and *SVP*

To identify regulators that mediate the regulation of class B and C genes by *SOC1*, *SVP*, and *AGL24*, we examined the expression of those known regulators of B and C class genes, including *LEUNIG* (*LUG*) (Liu and Meyerowitz, 1995), *SEUSS* (*SUE*) (Franks et al., 2002), and *SEP3* (Castillejo et al., 2005), and found that only *SEP3* expression was ectopically expressed in both vegetative and inflorescence apices of the triple mutants (Figure 2A; data not shown). In addition, we found that among all the floral homeotic genes tested, only *SEP3* was significantly upregulated in leaves and shoot apices of 9-day-old *soc1-2 agl24-1 svp-41* seedlings at the floral transitional stage (Figure 2B). Further examination of 6-day-old seedlings revealed that *SEP3* was upregulated in *svp-41*, and further strengthened in *soc1-2 svp-41* (Figure 3A). As *AGL24* was mainly expressed in the shoot apices of young seedlings (Liu et al., 2008), its loss-of-function effect on *SEP3* was not observed in whole seedlings. On the contrary, overexpression of *SOC1*, *SVP*, or *AGL24* all significantly suppressed *SEP3* in both leaves and shoot apices (Figure 3B).

We further compared *SEP3* expression in inflorescence apices of various mutants. In wild-type plants, *SEP3* expression was first detected in the upper portion of late stage 2 floral meristems (Mandel and Yanofsky, 1998), which was comparable with its expression in *soc1-2 svp-41* and *soc1-2 agl24-1* (Figures 3C–3E and Figure S6). In *agl24-1 svp-41*, ectopic *SEP3* expression was observed in stage 1 and 2 floral meristems of just bolting inflorescences, but not in the inflorescences 10 cm in height (Figures 3F and 3G and Figure S6). In *soc1-2 agl24-1 svp-41*, ectopic *SEP3* expression was detectable in apical meristems and stage 1 floral meristems of just bolting inflorescences, and turned stronger in apical meristems of the inflorescences 10 cm in height, especially in floral anlagen (Figures 3H and 3I; Figure S6). The trend of changes in *SEP3* expression patterns in bolting inflorescences was well correlated with the phenotype of *agl24-1 svp-41* or *soc1-2 agl24-1 svp-41*, as floral defects were alleviated acropetally in the former, while aggravated in the latter (Table S1). These observations show that *SEP3* is redundantly repressed by *SOC1*, *SVP*, or *AGL24* and indicate that ectopic expression of *SEP3* may contribute to the floral defects in *soc1-2 agl24-1 svp-41*.

SOC1, *AGL24*, and *SVP* Repress *SEP3* via Binding to a Common Promoter Region

We performed further ChIP assays to examine whether *SOC1*, *AGL24*, and *SVP* directly control *SEP3* expression. We scanned the *SEP3* genomic sequence for the CC(A/T)$_6$GG (CArG) motif,

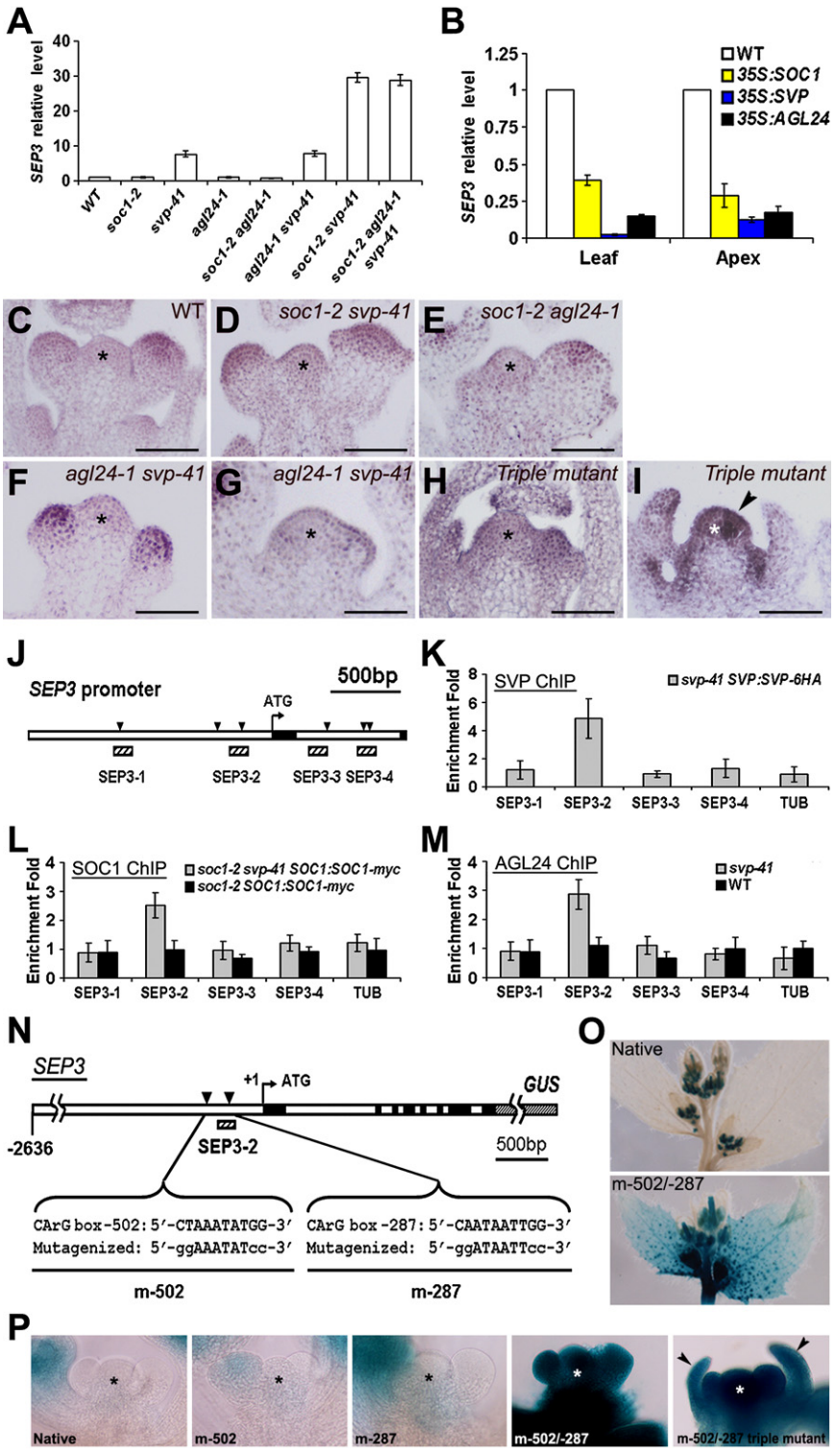

Figure 3. *SEP3* Is Repressed by *SVP*, *AGL24*, and *SOC1*

(A and B) *SEP3* expression in 6-day-old mutants (A) or overexpression transgenic seedlings (B). Plant tissues in (B) were dissected as described in Figure 2B. The *SEP3* expression level in wild-type is set as 1. Error bars indicate SD.

(C–E) In situ localization of *SEP3* expression in inflorescence apices of wild-type (C), *soc1-2 svp-41* (D), and *soc1-2 agl24-1* (E) plants. In these plants, *SEP3* expression pattern remains consistent in inflorescences in different heights.

(F–I) In situ localization of *SEP3* expression in inflorescence apices of *agl24-1 svp-41* (F and G) and *soc1-2 agl24-1 svp-41* (H and I). (F and H) Apices of just bolting inflorescences. (G and I) Apices of the inflorescences 10 cm in height. The arrowhead in (I) indicates strong *SEP3* expression in a floral anlagen. Asterisks in (C)–(I) indicate inflorescence meristems. Scale bars in (C)–(I), 100 μm.

(J) Schematic diagram of the *SEP3* promoter. The bent arrow indicates a translational starting site. Exons and introns are shown by black and white boxes, respectively. The arrowheads indicate the sites containing either one mismatch or perfect match from the consensus binding sequence (CArG box) for MADS domain proteins. The hatched boxes represent the DNA fragments amplified in ChIP assays.

(K) ChIP analysis of SVP binding to the *SEP3* promoter. Inflorescence apices of *svp-41 SVP:SVP-6HA* (Li et al., 2008) were harvested for the ChIP assay.

(L) ChIP analysis of SOC1 binding. Inflorescence apices of *soc1-2 SOC1:SOC1-myc*, which exhibited phenotypes like wild-type plants, were harvested for the ChIP assay. To test whether SVP affects SOC1 binding, a ChIP assay of *soc1-2 svp-41 SOC1:SOC1-myc* was also performed.

(M) ChIP analysis of AGL24 binding. Inflorescence apices of wild-type plants were harvested for the ChIP assay. To test whether SVP affects AGL24 binding, a ChIP assay of *svp-41* was also performed.

(N) Schematic diagram of the *SEP3:GUS* construct where a 4.7 kb *SEP3* genomic fragment including its coding region was fused with the *GUS* gene. Two native CArG boxes near SEP3-2 were mutated as indicated.

(O) GUS staining of inflorescence apices of the transformants containing *SEP3:GUS* (top panel) and its mutated construct (bottom panel).

(P) A close-up comparison of GUS staining of inflorescence apices of the transformants containing *SEP3:GUS* and various mutated constructs. Arrowheads in the last picture indicate bracts subtending floral meristems in *soc1-2 agl24-1 svp-41*. Asterisks indicate inflorescence meristems.

a canonical binding site for MADS domain proteins, with a maximum of one nucleotide mismatch and designed primers near the identified motifs for measurement of DNA enrichment (Figure 3J). SVP-6HA was associated with the region near the SEP3-2 fragment (Figure 3K), while SOC1-myc and AGL24 were only associated with the same region in the absence of SVP (Figures 3L and 3M). This indicates that *SVP* is a primary suppressor of *SEP3*, while *SOC1* and *AGL24* function redundantly. This is consistent with the expression analysis showing that *SVP* had the strongest effect on suppressing *SEP3* (Figures 3A and 3B).

To test in vivo whether two CArG motifs near SEP3-2 serve as binding sites of SVP, SOC1, and AGL24 for repressing *SEP3*

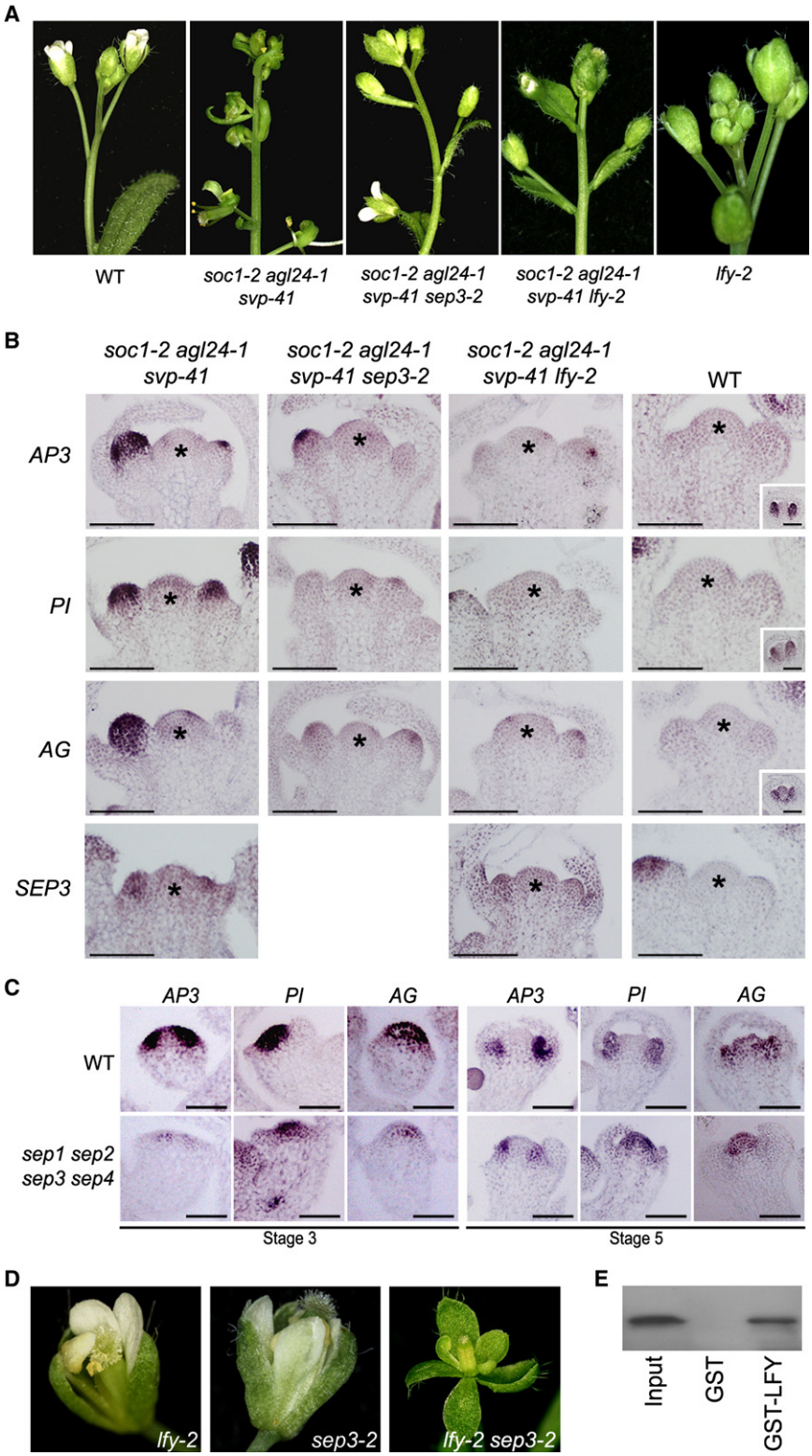

Figure 4. Floral Defects of *soc1-2 agl24-1 svp-41* Are Dependent on *SEP3* and *LFY*

(A) Floral defects of *soc1-2 agl24-1 svp-41* are partially rescued by *sep3-2* or *lfy-2*.

(B) Ectopic expression of *AP3*, *PI*, and *AG* in *soc1-2 agl24-1 svp-41* is suppressed by *sep3-2* or *lfy-2*. Insets show the expression of floral homeotic genes in wild-type stage 5 flowers. Asterisks indicate inflorescence meristems. Scale bars, 100 μm.

(C) Expression of *AP3*, *PI*, and *AG* in stage 3 and 5 flowers of wild-type and *sep1 sep2 sep3 sep4* plants. Scale bars, 100 μm.

(D) Synergistic effect of *lfy-2* and *sep3-2* on flower development.

(E) In vitro GST pull-down assay with LFY and SEP3 proteins. HA-tagged SEP3 produced by in vitro translation was incubated with immobilized GST or GST-LFY, respectively. Input, 5% in vitro translation product. Immunoblot analysis was performed using anti-HA antibody.

(Figure 3J), we created *SEP3:GUS* and its derived mutant constructs, in which two CArG motifs near SEP3-2 were mutagenized (Figure 3N). Transgenic plants bearing *SEP3:GUS* exhibited a staining pattern similar to that of endogenous *SEP3* expression (Figures 3O and 3P). In most of transgenic lines generated, mutagenesis of single CArG motif (m-502 or m-287) did not alter the GUS staining pattern, while mutagenesis of two CArG motifs (m-502/-287) caused dramatic ectopic GUS staining in whole plants including inflorescence apices (Figures 3O and 3P). Furthermore, introducing the m-502/-287 reporter line into *soc1-2 agl24-1 svp-41* did not enhance GUS staining (Figure 3P). These observations suggest that SVP, SOC1, and AGL24 specifically bind to both CArG motifs near SEP3-2 to repress *SEP3* expression.

Ectopic *SEP3* Activity Results in Ectopic Expression of Class B and C Genes

To test whether ectopic *SEP3* expression is relevant to ectopic expression of class B and C genes in *soc1-2 agl24-1 svp-41*, we created *soc1-2 agl24-1 svp-41 sep3-2*. This mutant exhibited significantly alleviated floral phenotypes (Figure 4A), indicating that *SEP3* contributes to the floral defects in *soc1-2 agl24-1 svp-41*.

As members of class E homeotic regulators, including SEP3, form protein complexes with other floral homeotic proteins to specify the floral organ identity (Honma and Goto, 2001), suppression of the floral defects in *soc1-2 agl24-1 svp-41* by *sep3-2* could be due to the removal of SEP3 from homeotic protein complexes rather than altered expression of class B and C genes. We thus compared the gene expression in *soc1-2 agl24-1 svp-41 sep3-2* and *soc1-2 agl24-1 svp-41*, and found that class B and C genes

were significantly downregulated in terms of scope and intensity in the quadruple mutants (Figure 4B). These results suggest that ectopic expression of class B and C genes induced by ectopic *SEP3* expression is responsible for the phenotypes in *soc1-2 agl24-1 svp-41*.

SEP Genes Activate the Expression of Class B and C Genes

The results from *soc1-2 agl24-1 svp-41* reminded us of a previous study showing ectopic activation of class B and C genes by overexpressing *SEP3* (Castillejo et al., 2005). Furthermore, initial *SEP3* expression in the apical region of late stage 2 floral meristems (Mandel and Yanofsky, 1998) covers the region where class B and C genes are activated (Goto and Meyerowitz, 1994; Jack et al., 1992; Yanofsky et al., 1990). These prompted us to hypothesize that *SEP3* together with other *SEP* genes may play a role in activating class B and C genes in wild-type plants.

The *SEP* family consists of four homologs in *Arabidopsis*. While their single mutants only exhibit subtle phenotypes, simultaneous loss of their function transforms all floral organs into leaf-like tissues (Ditta et al., 2004; Pelaz et al., 2000), demonstrating a crucial and redundant role of *SEP* genes in flower development. In situ hybridization revealed significantly reduced expression of class B and C genes at early stage 3 floral meristems of *sep1 sep2 sep3 sep4* (Figure 4C; Figure S7B). In stage 5 floral meristems of *sep1 sep2 sep3 sep4*, the expression domain of *AP3* or *AG* was restricted to a smaller region, while *PI* was completely misexpressed in the center of the meristems (Figures 4C; Figure S7B). Notably, the expression of the well-known activator of floral homeotic genes, *LFY*, was not altered in *sep1 sep2 sep3 sep4* (Figure S7A). These results indicate that *SEP* genes are required for activating the expression of class B and C genes at early stages even in the presence of *LFY*.

SEP3 and *LFY* Act in Concert to Activate the Expression of Class B and C Genes

We noticed that in *soc1-2 agl24-1 svp-41*, although *SEP3* was ectopically expressed in whole seedlings, class B and C genes were not expressed only until the emergence of floral primordia (Figure 2). This result implies that *SEP3* requires certain floral-specific cofactor(s) in activating class B and C genes. *LFY* is the most possible coregulator, because of its known function in activating class B and C genes and its expression throughout young floral meristems (Parcy et al., 1998; Weigel et al., 1992). In *soc1-2 agl24-1 svp-41*, *LFY* was highly expressed in emerging floral meristems (Figure S8), where *SEP3* was also ectopically expressed (Figures 2A, 3H, and 3I). To investigate whether transcriptional activation of class B and C genes by *SEP3* is dependent on *LFY*, we crossed *soc1-2 agl24-1 svp-41* with *lfy-2*, in which *LFY* function was partially lost (Schultz and Haughn, 1993). In *soc1-2 agl24-1 svp-41 lfy-2*, ectopic expression of class B and C genes was greatly reduced (Figure 4B). Accordingly, *soc1-2 agl24-1 svp-41 lfy-2* showed significantly rescued floral phenotypes as compared with *soc1-2 agl24-1 svp-41* (Figure 4A). These results suggest that *SEP3* and *LFY* function in concert in activating the expression of class B and C genes in *soc1-2 agl24-1 svp-41*.

To further test the concerted effect of *SEP3* and *LFY* on flower development, we created *lfy-2 sep3-2*. Flower development was almost normal in *sep3-2*, while *lfy-2* showed mild defects with a slightly reduced number of petals and stamens (Figure 4D). On the contrary, *lfy-2 sep3-2* showed dramatic floral defects, such as loss of most floral organs and homeotic transformation of stamens and petals into leaf-like structures (Figure 4D), confirming that *LFY* and *SEP3* synergistically act to regulate class B and C genes. This raises the possibility of direct interaction between LFY and SEP3, which was supported by a GST pull-down assay showing their physical interaction in vitro (Figure 4E).

SOC1 and AGL24 Interact with SAP18

We further sought to elucidate how *SVP*, *SOC1*, and *AGL24* repress *SEP3* expression. Protein sequence alignment revealed a conserved C-terminal motif in SOC1, SVP, AGL24, and another MADS box protein, AGL15 (Figure 5A). This conserved C-terminal motif, together with the K domain, of AGL15 was found to mediate the interaction between AGL15 and SAP18, a member of Sin3/HDAC complex (Hill et al., 2008; Silverstein and Ekwall, 2005). Thus, we tested whether SVP, SOC1, and AGL24 could also interact with SAP18. A GST pull-down assay revealed that SAP18 interacted with both SOC1 and AGL24, but not SVP (Figure 5B). Coimmunoprecipitation analyses further showed the in vivo interaction of SOC1 and AGL24 with SAP18 (Figures 5C and 5D). Moreover, bimolecular fluorescence complementation (BiFC) analysis, which detects protein-protein interactions through monitoring the fluorescence emitted by reconstitution of an enhanced yellow fluorescent protein from two fragments fused to two interacting proteins, revealed the direct interaction of SAP18-SOC1 (Figure 5E) and SAP18-AGL24 (Figure 5F) in the nuclei of living plant cells. These results strongly suggest that AGL24 and SOC1 interact with SAP18 in the nuclei. As mutating the conserved C-terminal motif only abolished the protein interaction between SAP18 and SOC1, but not AGL24 (Figures 5G and 5H), AGL24 interaction with SAP18 might rely on other domain(s) rather than the C-terminal motif.

Interaction of AGL24 and SOC1 with SAP18 raises the possibility that both SOC1 and AGL24 may repress *SEP3* transcription by recruiting an HDAC complex. We therefore analyzed histone acetylation status at the *SEP3* locus in various mutants. In general, hyperacetylation of histone H3 and H4 is associated with promoter regions of actively transcribed genes (Li et al., 2007). For *SEP3* chromatin, histone H3, but not H4, was hyperacetylated in *soc1-2 svp-41* and *soc1-2 agl24-1 svp-41* seedlings (Figure S9), in which *SEP3* was highly expressed (Figure 3A). This observation, together with the ChIP results (Figures 3L and 3M), supports the role of SOC1 and AGL24 in preventing H3 acetylation of *SEP3* in the absence of SVP.

As SAP18 did not interact with SVP, these two proteins may involve different mechanisms to repress *SEP3* transcription. To test this, we created *SAP18* knockdown lines by artificial microRNA interference (Schwab et al., 2006), and crossed a representative *AmiR-sap18* line with *svp-41*. As expected, *svp-41 AmiR-sap18* had higher *SEP3* expression than *svp-41* and *AmiR-sap18* (Figure 5I). Consequently, *svp-41 amiR-sap18* exhibited significant floral defects (Figure 5J), which partially mimicked those of *soc1-2 agl24-1 svp-41*. We further found that H3 acetylation of *SEP3* in *AmiR-sap18* increased in the *svp-41* background (Figure S9). These results suggest that

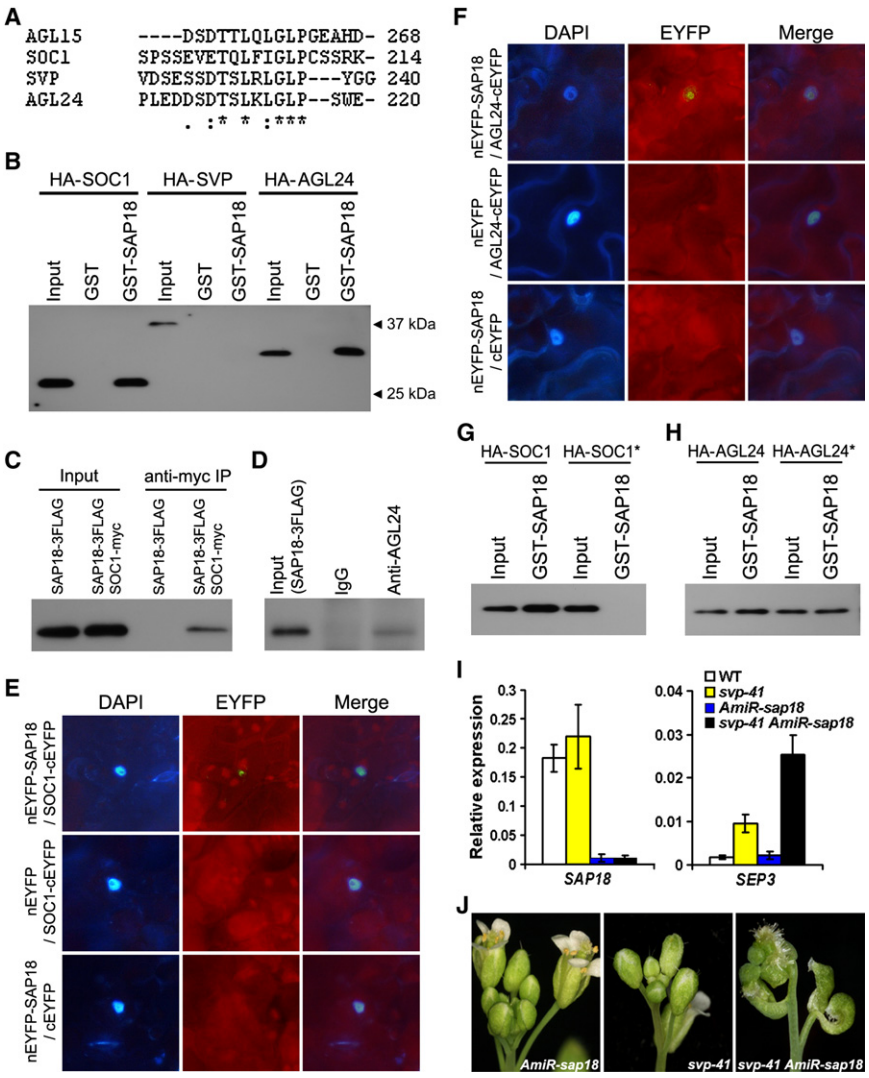

Figure 5. SOC1 and AGL24 Interact with SAP18

(A) Alignment of the conserved C-terminal motifs of SOC1, SVP, AGL24, and AGL15. Identical or less conserved amino acids residues are marked with asterisks or dots, respectively.

(B) In vitro GST pull-down assays. HA-tagged SOC1, SVP, and AGL24 produced by in vitro translation were incubated with immobilized GST or GST-SAP18, respectively. Input, 5% in vitro translation product. Immunoblot analysis was performed using anti-HA antibody.

(C) In vivo interaction between SAP18 and SOC1. Plant nuclear extracts from *35S:SAP18-3FLAG* and *35S:SAP18-3FLAG SOC1:SOC1-myc* were immunoprecipitated by anti-myc agarose beads. The coimmunoprecipitated protein was detected by anti-FLAG antibody.

(D) In vivo interaction between SAP18 and AGL24. Plant nuclear extracts from *35S:SAP18-3FLAG* were immunoprecipitated by either anti-AGL24 serum or preimmune serum (IgG). The coimmunoprecipitated protein was detected by anti-FLAG antibody.

(E and F) BiFC analysis of the interaction between SAP18 and SOC1 (E) or AGL24 (F). DAPI, fluorescence of 4′,6-diamino-2-phenylindol; EYFP, fluorescence of enhanced yellow fluorescent protein; Merge, merge of DAPI and EYFP.

(G and H) GST pull-down assay of the function of C-terminal motifs on the interaction between SAP18 and SOC1 (G) or AGL24 (H). In SOC1*, the C-terminal motif, LFIGL, was mutated into AFAGA (G), while in AGL24*, LKLGL was mutated into AKAGA (H). Immunoblot analysis was performed using anti-HA antibody.

(I) Downregulation of *SAP18* further derepresses *SEP3* expression in *svp-41*. Expression levels of *SAP18* and *SEP3* in 6-day-old seedlings were normalized against those of *TUB2*. Error bars indicate SD.

(J) Downregulation of *SAP18* in *svp-41* results in loss of floral organs and generation of carpelloid structures.

SAP18 recruited by AGL24 and SOC1 contributes to H3 deacetylation of *SEP3* in the absence of *SVP*.

SVP Interacts with TFL2

To understand how *SEP3* is repressed by SVP, we performed yeast two-hybrid screening to identify its protein partners. By using the SVP sequence as a bait, we found the sequences encoding TFL2/LHP1, the only *Arabidopsis* homolog of HP1 of metazoans and S. *prombe* (Gaudin et al., 2001; Kotake et al., 2003). Previous studies have suggested that *TFL2* suppresses genes involved in various developmental processes by recognizing H3K27me3 (Larsson et al., 1998; Turck et al., 2007; Zhang et al., 2007). In yeast TFL2 interacted with SVP but not its closest homolog AGL24 (Figure 6A). The interaction between SVP and TFL2 was confirmed by GST pull-down assays (Figures 6B and 6C). Their interaction required the chromoshadow domain of TFL2 and the conserved C-terminal motif of SVP (Figures 6A and 6D and Figure S10). BiFC analysis further revealed in vivo interaction of these two proteins in the nuclei (Figure 6E). These results suggest that SVP interacts with TFL2 in the nuclei.

To investigate the role of SVP in guiding TFL2 to the *SEP3* promoter, we performed ChIP analysis using *35S:TFL2-3HA* transgenic lines, which fully rescued *tfl2-1* loss-of-function mutants (data not shown). In agreement with previous data of genome-wide analysis of TFL2 binding (Zhang et al., 2007), we found that TFL2-3HA was associated with the *SEP3* locus (Figure 6F). Importantly, TFL2-3HA and SVP-6HA bound to the same genomic region (SEP3-2) with the highest enrichment fold (Figures 3K and 6F). In *svp-41*, the enrichment of TFL2-3HA binding to SEP3-2 was significantly decreased (Figure 6F). These results demonstrate that SVP plays an important role in guiding TFL2 to the SEP3-2 region.

We further found that H3K27me3 at the *SEP3* locus was almost completely lost in *tfl2-1* (Figure S11). This may partly explain the significantly increased *SEP3* expression in *tfl2* (Kotake et al., 2003), indicating that TFL2 represses *SEP3* by modulating H3K27me3. In *svp-41*, where localization of TFL2 to the *SEP3* locus was partially compromised, H3K27me3 at the *SEP3* locus was also reduced (Figure S11). Thus, SVP at least guides TFL2 to the *SEP3* locus, repressing *SEP3* by influencing H3K27me3.

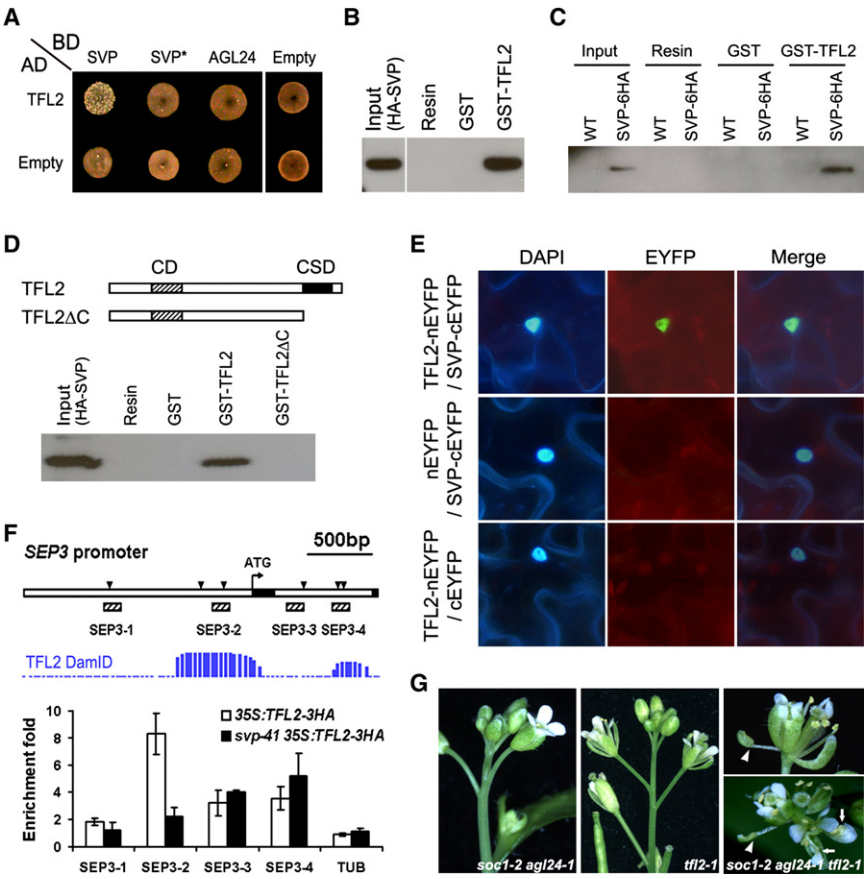

Figure 6. SVP Interacts with TFL2

(A) A yeast two-hybrid assay shows the interaction between SVP and TFL2. Transformed yeast cells grew on SD−His/−Trp/−Leu medium. In SVP*, the C-terminal motif, LRLGL, was mutated into ARAGA.

(B) In vitro GST pull-down assay with SVP and TFL2 proteins. HA-tagged SVP was incubated with immobilized GST or GST-TFL2, respectively. Resin, beads without any protein immobilized. Input, 5% in vitro translation product.

(C) A GST pull-down assay of the interaction of TFL2 and SVP-6HA in *svp-41 SVP:SVP-6HA*. Beads with or without proteins (GST or GST-TFL2) immobilized were incubated with protein extracts from 6-day-old *svp-41 SVP:SVP-6HA* plants.

(D) The interaction between TFL2 and SVP is mediated by the C-terminal portion of TFL2. A GST pull-down assay was performed as described in (B). Hatched or filled boxes represent the chromo domain (CD) or the chromoshadow domain (CSD) in TFL2, respectively. Immunoblot analyses in (B)–(D) were performed using anti-HA antibody.

(E) BiFC analysis of the interaction between SVP and TFL2.

(F) ChIP analysis of TFL2-3HA binding to the *SEP3* promoter. Inflorescence apices of *35S:TFL2-3HA* and *svp-41 35S:TFL2-3HA* were harvested for the ChIP assay. Genome-wide analysis of TFL2 binding via DNA adenine methyltransferase identification coupled with microarray (DamID-chip) method (http://epigenomics.mcdb.ucla.edu/H3K27m3) shows the similar binding regions in *SEP3* as revealed in this study. Error bars indicate SD.

(G) *soc1-2 agl24-1 tfl2-1* exhibits homeotic transformation of floral organs. The side view of *soc1-2 agl24-1 tfl2-1* flowers (upper panel) shows a sepaloid stamen (arrowhead), while the top view of the same structure (lower panel) shows additional stamenoid petals (arrows).

As SVP function is associated with TFL2, we reasoned that lack of TFL2 in *soc1-2 agl24-1* might produce certain floral phenotypes like those in *soc1-2 agl24-1 svp-41*. *soc1-2 agl24-1 tfl2-1* showed an enhanced determinate inflorescence with only two or three terminal flowers. These flowers developed sepaloid stamens and stamenoid petals in outer two whorls (Figure 6G), indicating the ectopic activity of class B and C genes. This result further supports that TFL2, which interacts with SVP, acts with SOC1 and AGL24 to regulate class B and C genes.

DISCUSSION

Control of Floral Patterning by Flowering Time Genes

Regulation of floral homeotic genes that specify floral organ identity is a key event for proper patterning of floral organs. Our findings have revealed a hitherto unknown genetic pathway that determines the timely expression of class B and C homeotic genes in floral meristems (Figure 7). The central regulators of this pathway are three MADS box transcription factors, *SVP*, *SOC1*, and *AGL24*, which were identified early as flowering time genes. These genes are redundantly required to prevent precocious expression of class B and C genes in emerging floral meristems through repression of *SEP3*. In floral meristems before late stage 2, class B and C genes are not expressed because *SEP3* is repressed by *SVP*, *SOC1*, and *AGL24*. As floral meristems proceed to late stage 2, direct repression of *SVP*, *SOC1*, and *AGL24* by the floral meristem identity gene *AP1* (Liu et al., 2007; Yu et al., 2004) gradually derepresses *SEP3*. Thus, in the apical region of early stage 3 floral meristems, *SEP3* and *LFY* function together to activate the expression of class B and C genes.

As *SEP3* is ectopically expressed in whole seedlings of *soc1-2 agl24-1 svp-41*, suppression of *SEP3* by *SVP*, *SOC1*, and *AGL24* is likely a constitutive event. This suppression in emerging floral meristems is vital for flower development, as it secures a normal expansion of floral anlagen into large floral meristems that contain sufficient cells for proper patterning of whorled organs by floral homeotic genes. Complete removal of this suppression in *soc1-2 agl24-1 svp-41* activates class B and C genes early in floral anlage, which in turn causes premature differentiation of floral meristems, thus producing a limited number of chimeric floral structures. In wild-type plants, *AP1* plays a progressive role in overcoming this suppression by repressing *SVP*, *SOC1*, and *AGL24* within a short, but crucial time window in young floral meristems before stage 3 (Liu et al., 2007; Yu et al., 2004). This leads to the timely derepression of *SEP3*, which in turn acts with *LFY* to activate class B and C genes in stage 3 floral meristems. Thus, consistent with previous studies showing concerted effects of *LFY* and *AP1* on regulating class B and C genes (Weigel et al., 1992; Weigel and Meyerowitz, 1993), our results propose a genetic pathway in which *AP1* contributes to floral

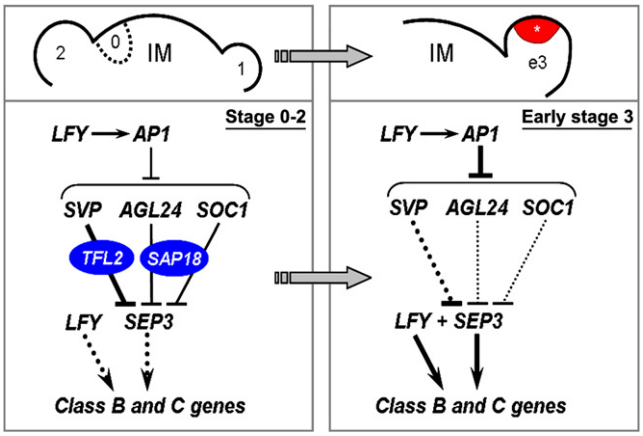

Figure 7. A Genetic Network of Early Floral Patterning

A genetic model shows that activation of floral homeotic gene expression requires the orchestrated regulation of *SEP3* by *SVP*, *SOC1*, and *AGL24* in emerging floral meristems. In floral anlagen and stage 1 and 2 floral meristems, class B and C homeotic genes are not activated by *LFY* alone, because its coregulator, *SEP3*, is repressed by *SVP*, *SOC1*, and *AGL24*, whose expression is directly mediated by *AP1*. To repress *SEP3*, SVP interacts with TFL2 to modulate H3K27me3, while SOC1 and AGL24 interact with SAP18 to modulate H3 acetylation. In early stage 3 (e3) floral meristem, strong repression of *SVP*, *SOC1*, and *AGL24* by *AP1* derepresses *SEP3*, which in turn functions with *LFY* to activate class B and C genes. The asterisk indicates the region where high *SEP3* expression coincides with initial expression of class B and C genes. Dotted lines or arrows indicate abolished regulation. The thickness of lines or arrows represents the strength of regulation. IM, inflorescence meristem.

patterning through regulation of the repression of *SEP3* by *SVP*, *SOC1,* and *AGL24*.

Transcriptional Activation of Class B and C Genes by *SEP3* and *LFY*

The class E floral regulators, including SEP3, have been suggested to form higher order protein complexes with other homeotic proteins to specify floral organ identity (Goto et al., 2001; Honma and Goto, 2001; Pelaz et al., 2000; Theissen, 2001). Our results suggest that *SEP3* plays an endogenous role in transcriptional regulation of class B and C genes in combination with *LFY*.

Although LFY interacts with SEP3 in vitro, our pull-down assays of GST-LFY and three other SEP proteins did not reveal any interaction (data not shown). SEP3 interaction with LFY could play dual roles in activating the expression of class B and C genes. First, *SEP3* provides more specific regional information for *LFY* function, because among all *SEP* genes, only *SEP3* is specifically expressed in the apical region of late stage 2 floral meristems where expression of class B and C genes is initiated, while *LFY* is expressed throughout the young floral meristems. Second, SEP3 protein has the strongest transcriptional activity among floral homeotic genes tested (Honma and Goto, 2001). Thus, SEP3 may enhance LFY transcriptional activation potential. Indeed, overexpression of *SEP3* and *LFY* exhibits phenotypes like those of the strong LFY:VP16, where LFY is fused to the strong activation domain of the viral transcription factor VP16 (Castillejo et al., 2005; Parcy et al., 1998). Therefore, orchestrated regulation of *SEP3* by *SVP*, *SOC1*, and *AGL24* in young floral meristems is indispensable for determining the timing for floral patterning.

Regulation of *SEP3* Expression by SOC1, AGL24, and SVP through Recruiting of Different Chromatin Factors

To unravel the underlying mechanisms by which *SEP3* is repressed by *SOC1*, *SVP*, and *AGL24*, we have demonstrated a typical scenario in which different chromatin factors relevant to various histone modifications are guided by three transcription factors to a specific locus. To maintain *SEP3* chromatin in a silenced state, SVP recruits TFL2 to modulate H3K27me3, while SOC1 and AGL24 interact with SAP18 to modulate histone acetylation in the absence of SVP (Figure 7).

Previous studies on TFL2 have suggested that it specifically associates with genome regions marked with H3K27me3 and is involved in maintaining gene repression (Turck et al., 2007; Zhang et al., 2007). *SEP3* has been identified as one of the potential targets of TFL2 through microarray and genome-wide ChIP analyses (Kotake et al., 2003; Zhang et al., 2007). Our results reveal the specific transcription factor, SVP, that plays a role in guiding the general chromatin factor TFL2 to the *SEP3* locus, thus repressing *SEP3* at least by affecting H3K27me3. Although comparison of H3K27me3 distribution in *Arabidopsis* Chromosome 4 in *tfl2* and wild-type plants has suggested that TFL2 may not be involved in the deposition of H3K27me3 (Turck et al., 2007), the mammalian homolog of TFL2, HP1, functions to not only decipher histone code, but it also encodes it (Kourmouli et al., 2005). H3K27me3 at the *SEP3* locus is almost completely lost in *tfl2-1*, and also reduced in *svp-41* where TFL2 binding to the *SEP3* locus is compromised (Figure S11), demonstrating a close link between TFL2 and the level of H3K27me3.

SAP18 is so far not well characterized, but is generally considered to be a structural protein that stabilizes the Sin3/HDAC complex and its interacting nonconstitutive components (Silverstein and Ekwall, 2005). SAP18 has been shown to interact with HDA19, an *Arabidopsis* histone deacetylase, and link the HDAC complex to transcriptional repressors that bind to specific chromatin regions (Hill et al., 2008; Song and Galbraith, 2006). In this study, we found that in the absence of SVP, SOC1 and AGL24 bind to the *SEP3* promoter, and their interaction with SAP18 modulates H3 acetylation at the *SEP3* locus, suggesting that SOC1 and AGL24 repress *SEP3* by recruiting the HDAC complex.

Coordinated repression of *SEP3* by *SOC1*, *SVP*, and *AGL24* through recruiting different chromatin factors demonstrates the flexibility of chromatin regulation during plant development. As *SEP3* is ultimately relevant to reproductive growth, it should be continuously repressed only until the conditions for flower development are appropriate. Although the expression trend of *SVP* is opposite to that of *SOC1* and *AGL24* during floral transition (Hartmann et al., 2000; Lee et al., 2000; Michaels et al., 2003; Yu et al., 2002), their capacity in recruiting different chromatin factors enables them to continuously create a nonpermissive chromatin environment for *SEP3* expression. This developmental plasticity allows plants to progress normally to the reproductive stage even if some of the redundant regulators are lost.

EXPERIMENTAL PROCEDURES

Plant Materials and Growth Conditions

All *Arabidopsis* plants were grown at 22°C under long days (16 hr light/8 hr dark). The mutants *soc1-2*, *svp-41*, *agl24-1*, *lfy-2*, *sep3-2*, and *tfl2-1* are in

Col background, while *ag-1* and *ap3-3* are in L*er* background. Except for transgenic plants harboring *35S:SAP18-3FLAG* that were selected on MS medium supplemented with kanamycin, transgenic plants with other constructs were selected by Basta on soil.

Plasmid Construction

To construct *SOC1:SOC1-myc*, the genomic fragment of *SOC1* was amplified as previously described (Liu et al., 2008), but with the sequence encoding a single myc incorporated into the reverse primer. The resulting PCR product was digested and cloned into pHY105 (Liu et al., 2007).

Genomic fragments of *SOC1*, *SVP*, and *AGL24* used for complementation experiments were described previously (Li et al., 2008; Liu et al., 2008). In the genomic fragments lacking the conserved C-terminal motif, the C-terminal 22, 22, and 21 amino acids of SOC1, SVP, and AGL24 were deleted from the intact genomic sequences, respectively.

To construct *SEP3:GUS*, a 4.7 kb *SEP3* genomic fragment was amplified with primers gSEP3-F-XmaI (5′-AACCCGGGTCCATCCAAATGGGACCTGTG-3′) and gSEP3-R-BamHI (5′-AAGGATCCAATAGAGTTGGTGTCATAAGGTA-3′) and cloned into HY107 (Liu et al., 2007). Based on this construct, mutations of the two CArG boxes near the SEP3-2 fragment were produced using QuikChange II XL-Site-Directed Mutagenesis Kit (Stratagene).

To construct *35S:SAP18-3FLAG*, the cDNA encoding *SAP18* was amplified with primers SAP18-FLAG-F (5′-CGTCGAAGCTCTGTCGTTCATGGCTGAAG CAGC GAGAAGACAAGG-3′) and SAP18-FLAG-R (5′-CATCGTCGTCCTTG TAGTCC ATGTAAATTGCCACATCCAGATAATCTCC-3′). The PCR product was digested and cloned into pCHF3-3FLAG (Yin et al., 2005).

To construct *AmiR-sap18*, design of artificial microRNA was performed according to the protocol published on the website (http://wmd2.weigelworld.org). Based on the gene submitted, a set of four primers was generated. After three rounds of PCR amplification, the resulting product was treated with EcoRI and BamHI, and cloned into pGreen-35S (Yu et al., 2004).

To construct *35S:TFL2-3HA*, the cDNA encoding for *TFL2* was amplified with primers TFL2-F2-XmaI (5′- CCCCCCGGGATGAAAGGGGCAAGTGGTG-3′) and TFL2-R3-SpeI (5′-GGACTAGTAGGCGTTCGATTGTACTTGA-3′) and cloned into pGreen-35S-3HA.

Expression Analysis

Total RNA was isolated with RNeasy Plant Mini Kit (QIAGEN) and reverse-transcribed with ThermoScript RT-PCR System (Invitrogen) according to the manufacturers' instructions. Real-time PCR was performed in triplicates on 7900HT Fast Real-Time PCR system (Applied Biosystems) with SYBR Green PCR Master Mix (Applied Biosystems). The relative expression level was calculated as previously reported (Liu et al., 2007). Nonradioactive in situ hybridization was performed as previously described (Liu et al., 2007). All primers sequences used for real-time PCR and the plasmids and primers used for synthesis of in situ probes are listed in Table S2.

Antibody Production

The peptide sequence DKLETLERAKLTTL from AGL24 was used for antibody production (1st base, Singapore). Anti-AGL24 antibody could specifically detect endogenous AGL24 in different genetic backgrounds (Figure S12A). To test whether anti-AGL24 could crosshybridize with SVP, the closest homolog of AGL24, we incubated anti-AGL24 antibody with HA-AGL24 or HA-SVP produced by TNT T7 Quick Coupled Transcription/Translation Systems (Promega). By tracing proteins with anti-HA antibody, we found that only HA-AGL24, but not HA-SVP, could be specifically immunoprecipitated by anti-AGL24 antibody (Figure S12B).

ChIP Assay

Plant materials were fixed on ice for 40 min in 1% formaldehyde under vacuum. Fixed tissues were homogenized, and chromatin was isolated and sonicated to produce DNA fragments around 500 bp as described (Liu et al., 2007). SOC1-myc, SVP-6HA, TFL2-3HA, and AGL24 protein was immunoprecipitated by anti-myc agarose conjugate (Sigma), anti-HA agarose conjugate (Sigma), and anti-AGL24 bound to Protein G PLUS agarose (Santa Cruz biotechnology), respectively. H3 and H4 acetylation and H3K27me3 were detected by anti-Acetyl-H3, anti-Acetyl-H4, and anti-H3K27me3 antibodies (Upstate Biotechnology), respectively. We performed three fully independent ChIP assays using samples collected separately. DNA enrichment was analyzed by quantitative real-time PCR in triplicates as previously reported (Li et al., 2008). The enrichment of a *Tubulin* (*TUB2*) genomic fragment was used as a negative control. All primers sequences used for ChIP assays are listed in Table S2.

Yeast Two-Hybrid Assay

The coding regions of *SVP*, *AGL24*, and *TFL2* were amplified and cloned into pGBKT7 and pGADT7 (Clontech), respectively. Subsequent yeast two-hybrid assays were carried out using the Yeastmaker Yeast Transformation System 2 according to the manufacture's instructions (Clontech). For library screening, BD-SVP was used as bait to screen an inflorescence cDNA library (CD4-30 from ABRC). Yeast transformants were selected on the SD medium lacking histidine, tryptophan, and leucine (SD−His/−Trp/−Leu) and supplemented with 0.2 mg/ml X-α-gal. The prey plasmids were recovered with the E.Z.N.A. Yeast Plasmid Kit (Omega Bio-Tek). For directly testing protein interactions, yeast *AH109* cells were cotransformed with specific bait and prey constructs, and plated onto the selective SD medium (SD−Trp/−Leu or SD−His/−Trp/−Leu).

In Vitro Pull-Down Assay

The cDNAs encoding *LFY*, *SAP18*, and *TFL2* were cloned into pGEX-4T-1 vector (Pharmacia). These expression vectors were transformed into *E. coli* Rosetta (DE3) (Novagen), and protein expression was induced by IPTG. The soluble GST fusion proteins were extracted and immobilized onto glutathione sepharose beads (Amersham Biosciences), and subsequently used for GST pull-down assays. HA-tagged SEP3, SOC1, SVP, and AGL24 proteins and their relevant mutant forms were synthesized as previously described (Li et al., 2008). These epitope-tagged proteins were incubated with the immobilized GST and GST fusion proteins. Proteins retained on the beads were resolved by SDS-PAGE and detected with anti-HA or anti-myc antibody (Santa Cruz Biotechnology).

Coimmunoprecipitation Experiments

Plant materials were harvested and nuclear proteins were extracted according to the ChIP protocol, but without tissue fixation. SOC1-myc or AGL24 protein was immunoprecipitated by anti-myc agarose conjugate (Sigma) or anti-AGL24 antibody bound to Protein G PLUS agarose (Santa Cruz biotechnology), respectively. Proteins bound by the beads were resolved by SDS-PAGE and detected by anti-FLAG antibody (Sigma).

BiFC Analysis

The cDNAs of SOC1, AGL24, SAP18, SVP, and TFL2 were cloned into serial pSAT1 vectors. The resulting cassettes including fusion proteins and constitutive promoters were cloned into pGreen binary vector HY105 and transformed into *Agrobacterium*. For BiFC experiments, 3-week-old tobacco (*Nicotiana benthamiana*) leaves were coinfiltrated with *Agrobacterium* as previously described (Sparkes et al., 2006).

SUPPLEMENTAL DATA

The Supplemental Data include twelve figures and two tables and can be found with this article online at http://www.cell.com/developmental-cell/supplemental/S1534-5807(09)00132-4.

ACKNOWLEDGMENTS

We thank P. Huijser, I. Lee, R. Amasino, M. Yanofsky, and K. Goto for various mutant seeds, S. Gelvin for pSAT1 vectors, Y. Yin for pCHF3-3FLAG, the Arabidopsis Biological Resource Center for the cDNA library (CD4-30), and T. Ito, F. Berger, and D. Jose for critical reading of the manuscript. This work was supported by Academic Research Funds T208B3113 from the Ministry of Education, Singapore, and R-154-000-282-112 from the National University of Singapore, and intramural research funds from Temasek Life Sciences Laboratory. L.C. was supported by the Singapore Millennium Foundation.

Received: December 12, 2008
Revised: February 20, 2009
Accepted: March 16, 2009
Published: May 18, 2009

REFERENCES

Bowman, J.L., Smyth, D.R., and Meyerowitz, E.M. (1991). Genetic interactions among floral homeotic genes of *Arabidopsis*. Development *112*, 1–20.

Castillejo, C., Romera-Branchat, M., and Pelaz, S. (2005). A new role of the *Arabidopsis* SEPALLATA3 gene revealed by its constitutive expression. Plant J. *43*, 586–596.

Coen, E.S., and Meyerowitz, E.M. (1991). The war of the whorls: genetic interactions controlling flower development. Nature *353*, 31–37.

Ditta, G., Pinyopich, A., Robles, P., Pelaz, S., and Yanofsky, M.F. (2004). The SEP4 gene of Arabidopsis thaliana functions in floral organ and meristem identity. Curr. Biol. *14*, 1935–1940.

Franks, R.G., Wang, C., Levin, J.Z., and Liu, Z. (2002). SEUSS, a member of a novel family of plant regulatory proteins, represses floral homeotic gene expression with LEUNIG. Development *129*, 253–263.

Gaudin, V., Libault, M., Pouteau, S., Juul, T., Zhao, G., Lefebvre, D., and Grandjean, O. (2001). Mutations in LIKE HETEROCHROMATIN PROTEIN 1 affect flowering time and plant architecture in *Arabidopsis*. Development *128*, 4847–4858.

Goto, K., and Meyerowitz, E.M. (1994). Function and regulation of the *Arabidopsis* floral homeotic gene PISTILLATA. Genes Dev. *8*, 1548–1560.

Goto, K., Kyozuka, J., and Bowman, J.L. (2001). Turning floral organs into leaves, leaves into floral organs. Curr. Opin. Genet. Dev. *11*, 449–456.

Gregis, V., Sessa, A., Colombo, L., and Kater, M.M. (2006). AGL24, SHORT VEGETATIVE PHASE, and APETALA1 redundantly control AGAMOUS during early stages of flower development in Arabidopsis. Plant Cell *18*, 1373–1382.

Gustafson-Brown, C., Savidge, B., and Yanofsky, M.F. (1994). Regulation of the arabidopsis floral homeotic gene APETALA1. Cell *76*, 131–143.

Hartmann, U., Hohmann, S., Nettesheim, K., Wisman, E., Saedler, H., and Huijser, P. (2000). Molecular cloning of SVP: a negative regulator of the floral transition in *Arabidopsis*. Plant J. *21*, 351–360.

Hill, K., Wang, H., and Perry, S.E. (2008). A transcriptional repression motif in the MADS factor AGL15 is involved in recruitment of histone deacetylase complex components. Plant J. *53*, 172–185.

Honma, T., and Goto, K. (2001). Complexes of MADS-box proteins are sufficient to convert leaves into floral organs. Nature *409*, 525–529.

Jack, T., Brockman, L.L., and Meyerowitz, E.M. (1992). The homeotic gene APETALA3 of *Arabidopsis thaliana* encodes a MADS box and is expressed in petals and stamens. Cell *68*, 683–697.

Kotake, T., Takada, S., Nakahigashi, K., Ohto, M., and Goto, K. (2003). *Arabidopsis* TERMINAL FLOWER 2 gene encodes a heterochromatin protein 1 homolog and represses both FLOWERING LOCUS T to regulate flowering time and several floral homeotic genes. Plant Cell Physiol. *44*, 555–564.

Kourmouli, N., Sun, Y.-M., van der Sar, S., Singh, P.B., and Brown, J.P. (2005). Epigenetic regulation of mammalian pericentric heterochromatin in vivo by HP1. Biochem. Biophys. Res. Commun. *337*, 901–907.

Larsson, A.S., Landberg, K., and Meeks-Wagner, D.R. (1998). The TERMINAL FLOWER2 (TFL2) gene controls the reproductive transition and meristem identity in *Arabidopsis thaliana*. Genetics *149*, 597–605.

Lee, H., Suh, S.S., Park, E., Cho, E., Ahn, J.H., Kim, S.G., Lee, J.S., Kwon, Y.M., and Lee, I. (2000). The AGAMOUS-LIKE 20 MADS domain protein integrates floral inductive pathways in *Arabidopsis*. Genes Dev. *14*, 2366–2376.

Lenhard, M., Bohnert, A., Jurgens, G., and Laux, T. (2001). Termination of stem cell maintenance in *Arabidopsis* floral meristems by interactions between WUSCHEL and AGAMOUS. Cell *105*, 805–814.

Li, B., Carey, M., and Workman, J.L. (2007). The role of chromatin during transcription. Cell *128*, 707–719.

Li, D., Liu, C., Shen, L., Wu, Y., Chen, H., Robertson, M., Helliwell, C.A., Ito, T., Meyerowitz, E., and Yu, H. (2008). A repressor complex governs the integration of flowering signals in Arabidopsis. Dev. Cell *15*, 110–120.

Liu, Z., and Meyerowitz, E.M. (1995). LEUNIG regulates AGAMOUS expression in *Arabidopsis* flowers. Development *121*, 975–991.

Liu, C., Zhou, J., Bracha-Drori, K., Yalovsky, S., Ito, T., and Yu, H. (2007). Specification of *Arabidopsis* floral meristem identity by repression of flowering time genes. Development *134*, 1901–1910.

Liu, C., Chen, H., Er, H.L., Soo, H.M., Kumar, P.P., Han, J.H., Liou, Y.C., and Yu, H. (2008). Direct interaction of AGL24 and SOC1 integrates flowering signals in *Arabidopsis*. Development *135*, 1481–1491.

Lohmann, J.U., Hong, R.L., Hobe, M., Busch, M.A., Parcy, F., Simon, R., and Weigel, D. (2001). A molecular link between stem cell regulation and floral patterning in *Arabidopsis*. Cell *105*, 793–803.

Mandel, M.A., and Yanofsky, M.F. (1998). The *Arabidopsis* AGL9 MADS box gene is expressed in young flower primordia. Sex. Plant Reprod. *11*, 22–28.

Mandel, M.A., Gustafson-Brown, C., Savidge, B., and Yanofsky, M.F. (1992). Molecular characterization of the *Arabidopsis* floral homeotic gene APETALA1. Nature *360*, 273–277.

Michaels, S.D., Ditta, G., Gustafson-Brown, C., Pelaz, S., Yanofsky, M., and Amasino, R.M. (2003). AGL24 acts as a promoter of flowering in *Arabidopsis* and is positively regulated by vernalization. Plant J. *33*, 867–874.

Ng, M., and Yanofsky, M.F. (2001). Activation of the *Arabidopsis* B class homeotic genes by APETALA1. Plant Cell *13*, 739–753.

Parcy, F., Nilsson, O., Busch, M.A., Lee, I., and Weigel, D. (1998). A genetic framework for floral patterning. Nature *395*, 561–566.

Pelaz, S., Ditta, G.S., Baumann, E., Wisman, E., and Yanofsky, M.F. (2000). B and C floral organ identity functions require SEPALLATA MADS-box genes. Nature *405*, 200–203.

Schultz, E.A., and Haughn, G.W. (1993). Genetic analysis of the floral initiation process (FLIP) in *Arabidopsis*. Development *119*, 745–765.

Schwab, R., Ossowski, S., Riester, M., Warthmann, N., and Weigel, D. (2006). Highly specific gene silencing by artificial microRNAs in *Arabidopsis*. Plant Cell *18*, 1121–1133.

Silverstein, R.A., and Ekwall, K. (2005). Sin3: a flexible regulator of global gene expression and genome stability. Curr. Genet. *47*, 1–17.

Smyth, D.R., Bowman, J.L., and Meyerowitz, E.M. (1990). Early flower development in *Arabidopsis*. Plant Cell *2*, 755–767.

Song, C.P., and Galbraith, D.W. (2006). AtSAP18, an orthologue of human SAP18, is involved in the regulation of salt stress and mediates transcriptional repression in *Arabidopsis*. Plant Mol. Biol. *60*, 241–257.

Sparkes, I.A., Runions, J., Kearns, A., and Hawes, C. (2006). Rapid, transient expression of fluorescent fusion proteins in tobacco plants and generation of stably transformed plants. Nat. Protocols *1*, 2019–2025.

Theissen, G. (2001). Development of floral organ identity: stories from the MADS house. Curr. Opin. Plant Biol. *4*, 75–85.

Theissen, G., and Saedler, H. (2001). Plant biology. Floral quartets. Nature *409*, 469–471.

Turck, F., Roudier, F., Farrona, S., Martin-Magniette, M.L., Guillaume, E., Buisine, N., Gagnot, S., Martienssen, R.A., Coupland, G., and Colot, V. (2007). *Arabidopsis* TFL2/LHP1 specifically associates with genes marked by trimethylation of histone H3 lysine 27. PLoS Genet. *3*, e86.

Wagner, D., Sablowski, R.W., and Meyerowitz, E.M. (1999). Transcriptional activation of APETALA1 by LEAFY. Science *285*, 582–584.

Weigel, D., and Meyerowitz, E.M. (1993). Activation of floral homeotic genes in *Arabidopsis*. Science *261*, 1723–1726.

Weigel, D., Alvarez, J., Smyth, D.R., Yanofsky, M.F., and Meyerowitz, E.M. (1992). LEAFY controls floral meristem identity in *Arabidopsis*. Cell *69*, 843–859.

Yanofsky, M.F., Ma, H., Bowman, J.L., Drews, G.N., Feldmann, K.A., and Meyerowitz, E.M. (1990). The protein encoded by the *Arabidopsis* homeotic gene agamous resembles transcription factors. Nature *346*, 35–39.

Yin, Y., Vafeados, D., Tao, Y., Yoshida, S., Asami, T., and Chory, J. (2005). A new class of transcription factors mediates brassinosteroid-regulated gene expression in *Arabidopsis*. Cell *120*, 249–259.

Yu, H., Xu, Y., Tan, E.L., and Kumar, P.P. (2002). AGAMOUS-LIKE 24, a dosage-dependent mediator of the flowering signals. Proc. Natl. Acad. Sci. USA *99*, 16336–16341.

Yu, H., Ito, T., Wellmer, F., and Meyerowitz, E.M. (2004). Repression of AGAMOUS-LIKE 24 is a crucial step in promoting flower development. Nat. Genet. *36*, 157–161.

Zhang, X., Germann, S., Blus, B.J., Khorasanizadeh, S., Gaudin, V., and Jacobsen, S.E. (2007). The *Arabidopsis* LHP1 protein colocalizes with histone H3 Lys27 trimethylation. Nat. Struct. Mol. Biol. *14*, 869–871.